



Effect of Inter-molecular Hydrogen Bond on ESIHT In 2, 2'-Dihydroxychalcone

Y. L. Ramu^{a*}, K. Jagadeesha^a, T. Shivalingaswamy^a, A. Raghu^a, M. Ramegowda^b

^{a*}PG Department of Physics, Govt. College (Autonomous), Mandya - 571401, INDIA.

^bphysics and Registrar (Admin.), Mandya University, Mandya-571401, INDIA.



CrossMark

Abstract

Micro properties such as ICT and ESIHT / ESIPT of bio-organic molecules require the theoretical study in addition to the experimental analysis. We adopted DFT / TDDFT along with PCM and EFP1 for the investigation of ground (S_0) and excited (S_1) state properties of 2,2'-dihydroxychalcone (DH) and its water complex $DH+(H_2O)_4-[DHH]$. An intra-molecular hydrogen bond exists between hydroxyl hydrogen and carbonyl oxygen in both DH and DHH molecules. Besides the intra-molecular hydrogen bond, in DHH four inter-molecular hydrogen bonds exist between DH and water molecules. The study of UV-Vis spectra both experimentally and theoretically reveals the S_1 state is predominant in both the gas and solvent phase. The optimization of molecules in the S_1 state resulted that the hydrogen atom transfuses from hydroxyl group to carbonyl group in DH molecule. The NBO analysis and potential energy scans confirm the hydrogen transfer at S_1 state of DH molecule. The hydrogen transfer is not observed in the excited state of DHH molecule due to the effect of inter-molecular hydrogen bond between water molecules and DH molecule.

Keywords: DH, DHH, DFT, TDDFT, PCM,EFP1, ESIHT

1. Introduction

The chalcones are important intermediates in the synthesis of flavonoids which are symbolized by their possession of a structure having two aromatic rings interconnected by a highly electrophonic carbon chain [1-2]. Generally, chalcones existed as chalcone O-glycosides and chalcone aglycones and they are widely apportioned in foods and beverages such as fruits, vegetables, soy-based foodstuff, spices and tea. Chalcones are available in mono and dicotyledonous plants, pteridophytes and gymnosperms but are synthesized as prime components in the families like Asteraceae and Aristolochiaceae [3]. The presence of α , β - unsaturated carbonyl group, chalcones and its derivatives exhibit diverse biological activities, namely antimicrobial, anti-inflammatory, antioxidant, antifungal, cytotoxic, antitumor, antimalarial, antiulcer, anticancer and antiviral [4-8]. Also, they have many applications such as artificial sweeteners [9], organic brightening agent, polymerization catalyst, fluorescent whitening agent [10]. Chalcones acquire conjugated double bonds and delocalized π -electron system on two benzene rings and they are used as intermediate for the synthesis of organic compounds of therapeutic value [11-13].

Hydroxychalcones are abundant in plants and they show many biological activities due to different sites of the hydroxyl group in the chalcone moiety and also, hydroxy chalcones on melanoma cells authenticated that the number of hydroxyl groups (-OH) in the molecule affects the power of their cytotoxic activity particularly isoliquiritigenin (ISLQ) had cytotoxic effects on neuroblastoma cells [14-16]. 4-hydroxychalcone shows the anti-angiogenic effect that may be beneficial in halting cancer spread [17]. 2',4'-dihydroxychalcone (DHC) is known to demonstrate antitumor activity in vitro [18]. Some derivatives of the chalcones such as xanthohumol and isobavachalcone show activity against anti-HIV-1, anti-bacterial, anti-cancer [19-21]. Elastichalcone B exhibits free radical scavenging inhibitory activity [22]. Some hydroxy chalcone derivatives also reveal strong inhibitory effects on the release of β -glucuronidase and lysozyme [23]. DH molecule is more potent due to activation of both rings by hydroxyl groups, originate to activate heat shock factor1 (Hsf1) and exhibited radiation sensitization characteristics in the colon and pancreatic cancer cells [24]. DH having a mechanism of antitumor activity in prostate cancer cells in vitro [25] and it is

*Corresponding author e-mail: ramuy/phy652@mail.com

Receive Date: 03 September 2021, Accept Date: 04 November 2021

DOI: 10.21608/EJCHEM.2021.94010.4428

©2022 National Information and Documentation Center (NIDOC)

one of the most effective chalcone for inducing NQO1[NAD(P)H: quinone reductase] and GST [glutathione S-transferase] [26-28].

Excited state intra-molecular hydrogen / proton transfer (ESIHT / ESIPT) has triggered the curiosity to understand the intrinsic mechanism implicated in chemical and biological processes [29-32] and also these reactions in the excited state attract a lot of attention in chemical and biological systems [33-37]. In optimized molecular structure having hydrogen-bonded system, hydrogen/proton transfer can be possible both in inter-molecular as well as intra-molecular [38-41]. ESIPT / ESIHT is one of the characteristic elementary chemical reactions which can occur due to photo-excitation. In these reactions, a proton is transferred from a donating hydroxyl group to an accepting carbonyl group [42].

The development of the EFP method for modeling hydrogen-bonded systems enacts a key role in studies of a wide extent of chemical and biological processes for the explicit treatment of solvent molecules. Out of two EFP methods EFP1 and EFP2, the original method EFP1, was initially evolved to explain aqueous solvation, by representing coulombic, induction and repulsive interactions [43-44]. Polarizable continuum model (PCM) is a solvation model for a Quantum Mechanical (QM) molecular system in which the solvent is symbolized as a continuum distribution of matter to describe the solvation effect on photo physical characteristics of biological and chemical chromophores at lower and higher energy states by implementing the DFT / TDDFT method [45-46].

2. Experimental

The pure DH sample was procured from Sigma-Aldrich, dissolved in aqueous methanol. Using Labtronics LT-291 UV-Vis spectrometer the absorption spectral properties of DH sample in aqueous methanol was performed. The absorption wavelength was found to be 370nm. The higher dilution does not change the peak value of the wavelength, only absorption intensity changes.

3. Computational schemes

The DH and DHH molecules were modeled using Avogadro molecular modeling package [47] and optimized with MMFF94s force field. Using the generated coordinates of the molecules from the Avogadro package, all required calculations have been performed using the NBO [48] unified GAMESS software suite [49-50]. The ground and first excited state optimization of DH and DHH molecules were carried out at the level of DFT / B3LYP [51-56] / TDDFT with B3LYP [57-59] hybrid functional with 6-31G (d,p) basis set. Based on optimized ground state geometry, vertical

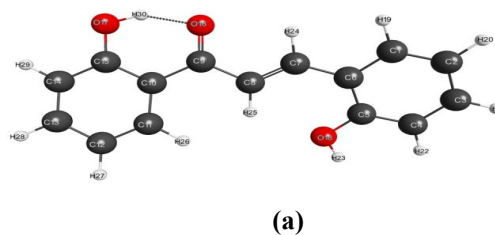
excitation and absorption energies were computed using TDDFT / B3LYP / 6-31G (d,p) / PCM / EFP1 method [60-64]. Natural charges were calculated lower (S_0) and higher energy (S_1) states by using the NBO method. Molecular orbitals and UV spectra were plotted using wxMacMolPlt and Gabedit.

4. Results and discussion

4.1 Structural properties at ground state

Optimized parameters like bond lengths, bond angles of DH and DHH molecules were obtained by employing 6-31G (d,p) basis set with B3LYP / DFT / TDDFT method and are showed in **Table -1 and 2**. By using the ground state optimized coordinates of DH / DHH molecules, one can plot frontier molecular orbital's, difference charge density map, electrostatic potential map and natural charges. The respective ground state optimized molecular structures and plots of electrostatic potential and difference electron density map are presented in the Fig.1 and natural charges are presented in the Table.3. In the ground state, we observed that one intra-molecular hydrogen bond O17-H30...O16=C9 arise between the oxygen of the carbonyl group and hydrogen of the 2'-hydroxyl group. The hydration to DH molecule using EFP1 method causes four inter-molecular HB's with four water molecules, two by 2-hydroxyl group (-O18H23) and other two in between by 2'-hydroxyl group (-O17H30) and carbonyl group (C9=O16) along with the HB between two water molecules. The hydration to the DH molecule slightly changes the structural parameters of the carbonyl group and hydroxyl groups due to the formation of inter-molecular HBs.

In the difference charge density map, red/blue zones of the molecular orbitals belong to ρ^-/ρ^+ respectively. Blue regions are established on C3, C6, C7, C10, C14, C15, O16, and red regions are established on the C1, C2, C4, C5, C8, C9, C12, C13, O17 atoms and O17 atom shows slightly negative charge than the O16 atom. The electrostatic potential map along with the natural charges on different atoms of the molecule shows that carbonyl and 2'-hydroxyl groups were more reactive for electrophiles and that on 2-hydroxyl group was less reactive for electrophiles. The plot of frontier molecular orbital's and difference electron density map elucidate that the electronic charge accumulated on the hydroxyl groups, carbonyl, alkyl chain and two benzene rings.



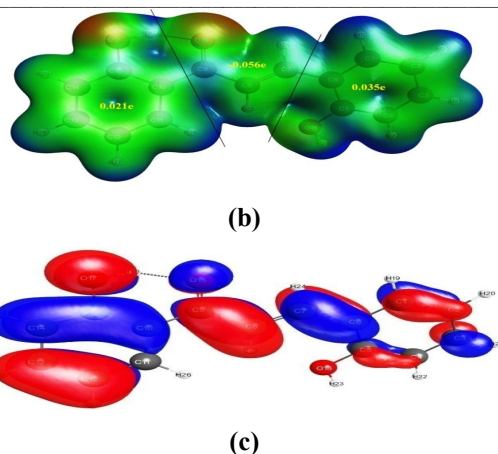


Fig.1: (a) optimized molecular structure (b) MEP along with natural charges on various groups and (c) Difference electron density map of DH molecule at S_0 state.

Table-1: Selected bond lengths between various atoms of DH / DHH molecules at S_0 , S_1 states optimized by 6-31G (d, p) / B3LYP method

r/(Å^0)	DH		DHH		$A(^{\circ})$
	S_0	S_1	S_0	S_1	
R(1-2)	1.39	1.384	1.389	1.385	A(1-2-3)
R(2-3)	1.396	1.401	1.397	1.401	A(2-3-4)
R(3-4)	1.393	1.397	1.393	1.399	A(3-4-5)
R(4-5)	1.398	1.393	1.4	1.391	A(4-5-6)
R(5-6)	1.418	1.431	1.418	1.434	A(5-6-1)
R(6-1)	1.41	1.426	1.411	1.427	A(6-7-8)
R(1-19)	1.087	1.087	1.087	1.087	A(8-9-10)
R(2-20)	1.085	1.086	1.085	1.086	A(9-10-15)
R(3-21)	1.086	1.086	1.086	1.086	A(10-11-12)
R(4-22)	1.088	1.089	1.087	1.089	A(11-12-13)
R(5-18)	1.365	1.367	1.355	1.365	A(12-13-14)
R(18-23)	0.967	0.967	0.965	0.963	A(13-14-15)
R(6-7)	1.457	1.424	1.455	1.423	A(14-15-10)
R(7-24)	1.089	1.088	1.089	1.088	A(14-15-17)
R(7-8)	1.351	1.393	1.354	1.406	A(8-9-16)
R(8-25)	1.079	1.08	1.078	1.08	A(10-9-16)
R(8-9)	1.476	1.397	1.472	1.391	A(10-15-17)
R(9-10)	1.476	1.514	1.472	1.539	
R(10-11)	1.412	1.369	1.415	1.366	
R(11-12)	1.385	1.443	1.385	1.452	
R(12-13)	1.404	1.375	1.404	1.38	

R(13-14)	1.385	1.411	1.386	1.399
R(14-15)	1.407	1.426	1.404	1.426
R(15-10)	1.427	1.436	1.428	1.421
R(11-26)	1.085	1.086	1.083	1.084
R(12-27)	1.085	1.085	1.085	1.085
R(13-28)	1.087	1.086	1.087	1.085
R(14-29)	1.085	1.085	1.085	1.083
R(15-17)	1.337	1.295	1.342	1.32
R(17-30)	0.999	-	0.997	1.064
R(9-16)	1.253	1.305	1.26	1.293
R(16-30)	-	1.101	-	-

Table 2: Selected bond angles between various atoms of DH / DHH molecules at S_0 , S_1 states optimized by 6-31G (d, p) / B3LYP method

$A(^{\circ})$	DH		DHH	
	S_0	S_1	S_0	S_1
119	120	119	120	
120	120	120	119	
121	121	121	121	
121	121	120	121	
117	116	117	116	
130	130	131	130	
120	124	121	122	
119	117	119	117	
122	122	121	121	
119	119	120	121	
121	120	121	119	
120	122	120	120	
120	118	120	121	
118	122	118	119	
120	122	119	126	
120	114	120	113	
122	121	122	120	

4.2 ICT states of the molecules

The simulation of UV-Vis spectra of DH and DHH molecules in the gaseous medium, water, and methanol solvents were executed at the level of TDDFT/ 6-31G(d,p) / B3LYP / PCM / EFP1method. The oscillator strength, absorption wavelengths, and possible wave function are tabulated in Table-4 and a spectrum is evinced in the Fig 2. On perceiving the

corresponding oscillator strengths, S_1 state of both DH and DHH were found to be more probable in gas phase to study ICT states. The calculated theoretical absorption wavelength for maximum oscillating strength in the gas phase, water, and methanol solvents are 381 nm, 378 nm and 378.2 nm for DH and 393 nm, 396 nm, 393 nm for DHH molecules respectively. A red shift observed in micro-solvated molecule indicates weakening of HBs in the excited states. The theoretical absorption wavelength of DH molecule in methanol solvent was found to be 377 nm is in good accord with the experimental value which is about 370 nm.

Using the ground state optimized co-ordinates, DH molecule were optimized at S_1 state. In the excited state, inter-molecular HB's slightly gets disturbed and also, the structural parameters were slightly altered particularly in hydroxyl groups and a carbonyl group. In the excited state of DH molecule, a hydrogen atom (H30) transpires from hydroxyl group to carbonyl group. The negative charge on hydroxyl oxygen O17 decreases and negative charge on carbonyl oxygen O16 increases in S_1 state of pure and its water complex. On observing the overall change in the natural charges of the 2'-hydroxyl (-O17H30) and carbonyl (-O16C9) groups of DH molecule, the negative charge on the 2'-hydroxyl group decreases and that on carbonyl group increases in the S_1 state. So hydrogen transfer can be observed in the S_1 state.

In DHH molecule, the negative charge on the 2'-hydroxyl group decreases and negative charge on the Carbonyl group increases to larger extent in S_1 . So, no hydrogen transfer can be observed in DHH molecule due to the effect of micro-solvation. The excited state optimized molecular structures along with the electrostatic potential maps were shown in the Fig.3 and natural charges were listed in the Table-3.

Table-3: Natural charges on various atoms of DH / DHH molecules at S_0 , S_1 states

		TDDFT / B3LYP / 6-31G(d,p)					
Molecule	State	Gas phase		Water		Methanol	
		λ_a	f	λ_a	f	λ_a	f
DH	S_1	381	0.205	378.3	0.478	378.2	0.471
		H→L(0.991)		H→L(-0.970)		H→L(0.986),	
				H-1→L(-0.209)		H-1→L(0.113)	
DHH	S_1	393.9	0.192	386	0.550	393.9	0.193
		H→L(0.986),		H→L(-0.971),		H→L(0.986),	
		H-1→L(0.113)		H-1→L(-0.183)		H-1→L(0.113)	

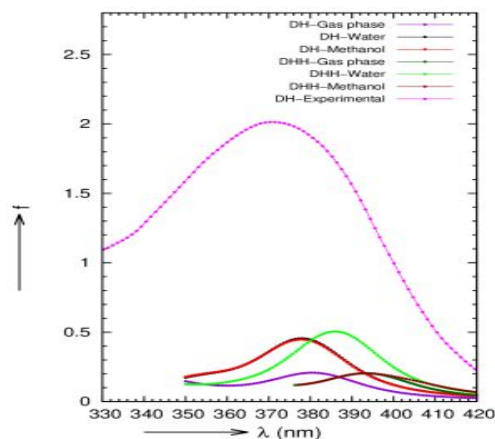
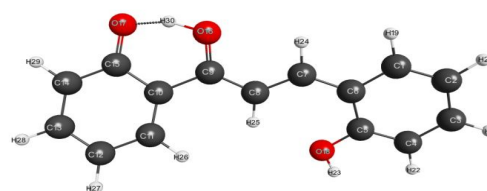
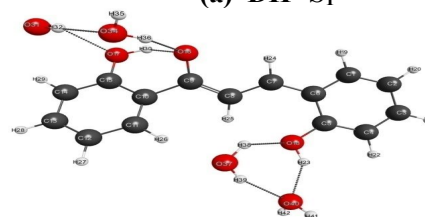


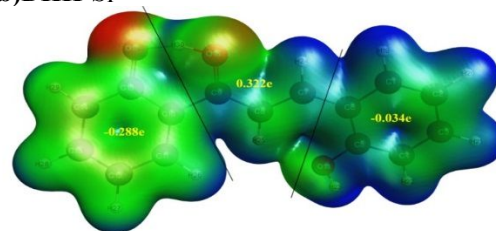
Fig.2: Experimental and theoretical simulated absorption spectra of DH and DHH molecules in gas phase, water and methanol solvents.



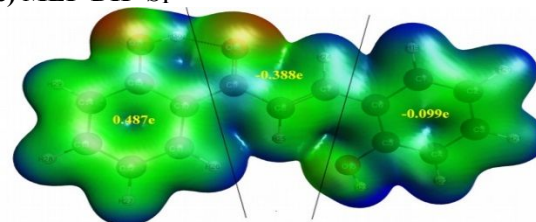
(a) DH- S_1



(b) DHH- S_1



(c) MEP-DH- S_1



(d) MEP-DHH- S_1

Fig.3: (a) and (b) Optimized molecular structure of DH /DHH molecules at S_1 state. (c) and (d) MEP along with natural charges on various groups of DH /DHH molecules at S_1 state.

Table-4: Absorption wavelength [λ (nm)] and oscillator strength (f) of DH and DHH molecules with probable transitions

Atom	DH		DHH	
	S ₀	S ₁	S ₀	S ₁
C1	-0.185	-0.192	-0.181	-0.205
C2	-0.265	-0.267	-0.269	-0.270
C3	-0.206	-0.221	-0.203	-0.239
C4	-0.320	-0.326	-0.320	-0.328
C5	0.365	0.361	0.368	0.346
C6	-0.135	-0.148	-0.140	-0.144
C7	-0.144	-0.137	-0.134	-0.167
C8	-0.310	-0.387	-0.316	-0.419
C9	0.522	0.489	0.530	0.452
C10	-0.222	-0.221	-0.222	-0.187
C11	-0.186	-0.117	-0.182	-0.142
C12	-0.280	-0.227	-0.294	-0.142
C13	-0.197	-0.249	-0.189	-0.287
C14	-0.295	-0.190	-0.295	-0.133
C15	0.397	0.379	0.397	0.404
O16	-0.625	-0.659	-0.684	-0.742
O17	-0.694	-0.658	-0.713	-0.652
O18	-0.693	-0.695	-0.744	-0.749
H19	0.245	0.240	0.244	0.235
H20	0.247	0.244	0.247	0.238
H21	0.246	0.242	0.245	0.235
H22	0.235	0.231	0.233	0.224
H23	0.501	0.498	0.576	0.557
H24	0.252	0.245	0.246	0.239
H25	0.250	0.255	0.250	0.249
H26	0.239	0.250	0.259	0.322
H27	0.242	0.245	0.247	0.250
H28	0.242	0.249	0.244	0.257
H29	0.253	0.252	0.255	0.270
H30	0.523	0.517	0.524	0.526

4.3 ESIHT process

The ESIHT mechanism occurs in the S₁ state of DH molecule due to charge transfer from 2'-hydroxyl group (O17H30) to a carbonyl group (C9O16) with the refashioning of intra-molecular HB O17-H30...O16=C9 to O17...H30-O16=C9. The ground / excited states potential energy surface (PES) scans of the H30 atom transferred route have been done with LR-TDDFT / B3LYP / 6-31G (d,p) method in the gas

phase. The PES plot Fig. 4 depicts the variation of potential energy with -OH bond (O17-H30) distance in DH molecule. In the plot, it is observed that the DH molecule can endure in "S₁^{*}" -state [un-relaxed first excited state] by photo-excitation with absorbed energy 3.22 eV, the O17-H30 (bond energy 3.45 eV) elongated to 1.645 Å the H30 atom disentangled from O17 and covalently bonded to O16. At this point the hydrogen atom (H30) exile from the 2'-hydroxyl group to the carbonyl group, hence ESIHT occurs. The DH molecule was frozen in the "S₁"-state [relaxed first excited state] with O16-H30 bond length of 1.101 Å. The molecule de-excited to "S₀^{*}"-state [un-relaxed ground state]. At this state the O16-H30 (bond energy 0.73 eV) the bond length in the DH molecule again stretches to 1.365 Å, where the expulsion of H30 atom from O16 to O17 takes place and the molecule come back to "S₀" [relaxed ground state].

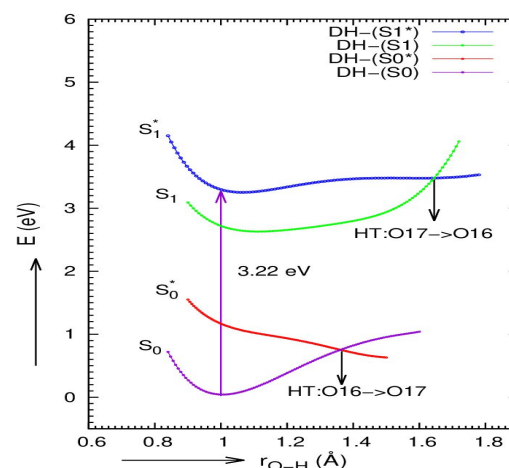


Fig.4: Potential energy plot along the hydrogen atom transfer path of DH molecule.

5. Conclusion

DFT and TDDFT calculations have been performed to investigate the intra-molecular hydrogen transfer mechanism in DH at S₁ state. The hydrogen transfer mechanism can be endorsed by potential energy surface scans, while in that of DHH hydrogen transfer reaction cannot take place in the excited state due to the effect of micro-solvation and can be endorsed by natural charge analysis. Electronic absorption wavelengths and congenial oscillator strengths of the low-lying, electronically excited states are computed using the TDDFT / EFPI / B3LYP / 6-31G(d,p) method in gas phase, water and methanol solvents which show different degrees of red-shift under the effect of micro-solvation which is facilitated by hydrogen-bond weakening in the excited state. There is a good agreement between theoretical and experimental electronic absorption

wavelengths for DH molecule in the methanol solvent.

6. Conflicts of interest

There are no Conflicts to declare.

7. References

- Sweetey S., Kumar K., Nepali S., Sapra O. P., Suri K.L., Dhar G.S., Sarma and Saxena A. K., Synthesis and Biological Evaluation of Chalcones having Hetero substituent(s). *Indian J Pharm Sci*, 72(6), 801-806(2010).
- Bhalara N., Kalariya J. and Dobariya N., Synthesis and Antimicrobial Screening of some Chalcones. *International Journal of Scientific Research and Reviews*, 7(1), 40-45(2018)
- Iwashina T., The structure and distribution of the flavonoids in plants. *J Plant Res*, 113(3), 287-299(2000).
- Dimmock J. R., Elias D. W., Beazely M. A. and Kandepu N. M., Bioactivities of chalcones. *Curr Med Chem*, 6(12), 1125-1149(1999).
- Go M. L., Wu X. and Liu X. L., An Update on Cytotoxic and Chemoprotective Properties. *Curr. Med. Chem.*, 12 (215), 483-499(2005).
- Satyanarayana and Rao M.N.A., Anti-inflammatory, analgesic and antipyretic activities of 3-(4-(3-(4-dimethylamino-phenyl)-1-oxo-2-propenyl) phenyl)sydnone. *Indian Drugs*, 30(7), 313-318(1993).
- Ballesteros J. F., Sanz M. J., Ubeda A., Miranda M. A., Iborra S., Paya M. and Alcaraz M. J., Synthesis and pharmacological evaluation of 2'-hydroxychalcones and flavones as inhibitors of inflammatory mediators generation. *J. Med. Chem*, 38 (14), 2794(1995).
- Hsieh H. K., Tsao L. T., Wang J. P. and Lin C. N., Synthesis and anti-inflammatory effect of chalcones. *J. Pharm. Pharmacol*, 52(2), 163-171(2000).
- Mousa AS. and Suhaib M., Synthesis, Characterization, and Reactions of Selected Multichalcone Derivatives. *J. Heterocyclic Chem*, 46, 201-206(2009).
- Vishwanadham Y., Kumaraswamy T., Suman D., Anusha V., Prathima P. and Samhitha T., A review on Chalcones and its importance. *PharmaTutor*, 1(2), 54-59(2013).
- Straub T. S., Epoxidation of α , β -unsaturated ketones with sodium perborate. *Tetrahedron Lett*, 36(5), 663-664(1995).
- Ankita A., Bhalu., Kapil D., Bhesaniya., Nayan J., Vekariya., Shipra H. and Baluja., Chalcones: A Solubility study at different temperatures. *International Letters of Chemistry, Physics and Astronomy*, 31, 7-19(2014).
- Gupta K. R., Badole S., Gupta J. K. and Singh, synthesis and screening for biological potential of some substituted chalcones. *International journal of pharmaceutical chemistry and analysis*, 5(2), 84-88(2018).
- Calliste C. A., le Bail J. C. and Trouillas P., et al., Chalcones: structural requirements for antioxidant, estrogenic and anti-proliferative activities. *Anticancer Research*, 21(6), 3949-3956(2001).
- Nerya O., Musa R., Khatib S., Tamir S. and Vaya J., Chalcones as potent tyrosinase inhibitors: the effect of hydroxyl positions and numbers. *Phytochemistry*, 65(10), 1389-1395(2004).
- Navarini A. L. F., Chiaradia L. D. and Mascarello A., et al., Hydroxychalcones induce apoptosis in B16-F10 melanoma cells via GSH and ATP depletion. *European Journal of Medicinal Chemistry*, 44(4), 1630-1637(2009).
- Varinska L., van Wijhe M. and Belleri M., et al., Anti-angiogenic activity of the flavonoid precursor 4-hydroxychalcone. *European Journal of Pharmacology*, 691(3), 125-133(2012).
- Sheng Y., Zou M., Wang Y. and Li Q., 2',4'-dihydroxychalcone, a flavonoid isolated from *Herba oxytropis*, suppresses PC-3 human prostate cancer cell growth by induction of apoptosis. *Oncology letters*, 10, 3737-3741(2015).
- Wang Q., Ding Z. H., Liu J. K. and Zheng Y. T., Xanthohumol, a novel anti-HIV-1 agent purified from Hops *Humulus lupulus*. *Antiviral Res*, 64(3), 189-194(2004).
- Inamori Y., Baba K., Tsujibo H., Taniguchi M. and Nakata k., 250 Kozawa, Antibacterial activity of two chalcones, xanthoangelol and 4-hydroxyderricin, isolated from the root of *Angelica keiskei koidzumi*. *Chem. Pharm*, 39, 1604-1605(1991).
- Harikumar K. B., Kunnumakkara A. B., Ahn K. S., Anand P., Krishnan S., Guha S., and Aggarwal B. B., Modification of the cysteine residues in IB kinase and NF-B (p65) by xanthohumol leads to suppression of NF-B-regulated gene products and potentiation of apoptosis in leukemia cells. *Blood First Edition paper*, 113, 2003-2013(2009).
- Ramli F., Rahmani M., Kassim N. K., Hashim N. M., Sukari M. A., Akim A. M. and Go R., New diprenylated dihydrochalcones from leaves of *Artocarpus elasticus*. *Phytochem. Lett*, 6(4), 582-585(2013).
- Lin C., Lee T. H., Hsu M. F., Wang J. P., Ko F. N. and Teng C. M., 2,5-Dihydroxychalcone as a Potent Chemical Mediator and Cyclooxygenase Inhibitor. *J. Pharm. Pharmacol*, 49, 530-

- 536(1997).
24. Pruitt R., Sasi N., Michael., Freeman., Konjeti R. and Sekhar, Radiosensitization of cancer cells by hydroxychalcones, *Bio-organic Medicinal Chemistry Letters*, 20, 5997-6000(2010).
 25. Ahmed Q., Haddad., Neil F., Colleen N., Basil S., Mireia M., Vasundara V. and Laurence Klotz., Antiproliferative Mechanisms of the Flavonoids 2,2'-Dihydroxychalcone and Fisetin in Human Prostate Cancer Cells. *Nutrition and Cancer*, 62(5), 668-681(2010).
 26. Dinkova-Kostava A. T., Massiah M. A., Bozak R. E., Hicks R. J., and Talalay P., 275 Potency of Michael reaction acceptors as inducers of enzymes that protect against carcinogenesis depends on their reactivity with sulfhydryl groups, *Proc. Natl. Acad. Sci.U.S.A.* 98, 3404-3409(2001).
 27. Miranda C. L., Aponso G. L. M., Stevens J. F., Deinzer M. L and Buhler D. R., Prenylated chalcones and flavanones as inducers of quinone reductase in mouse Hepa 1c1c7 cells. *Cancer Lett*, 149(1-2), 21-29(2000).
 28. Fiander H. and Schneider H., Dietary ortho phenols that induce glutathione S-transferase and increase the resistance of cells to hydrogen peroxide are potential cancer chemopreventives that act by two mechanisms: the alleviation of oxidative stress and the detoxification of mutagenic xenobiotics. *Cancer Lett*, 156(2), 117-124(2000).
 29. Jagadeesha K., Ramu Y. L., Ramegowda M. and Lokanath N. K., Excited state hydrogen atom transfer in micro-solvated dicoumarol: A TDDFT / EFP1 study. *Spectrochim.ActaA*, 208, 325-330(2018).
 30. Meyer T. J., Huynh M. H. V. and Thorp H. H., Theoretical Study of Electron, Proton, and Proton-Coupled Electron Transfer in Iron Bimimidazole Complexes. *J. Am. Chem. Soc.* 123(16), 3723-3733(2001).
 31. Hammes-Schiffer S., Introduction: Proton-Coupled Electron Transfer. *Chem. Rev*, 110, 6937-1938(2010).
 32. Ramegowda M., Ranjitha K. N. and Deepika T. N., Exploring excited state properties of 7-hydroxy and 7-methoxy 4-methylcoumarin: a combined time-dependent density functional theory/effective fragment potential study. *New J. Chem.*, 40(3), 2211-2219(2016).
 33. Liu Y. H., Lan S. C., Zhu C. and Lin S. H., Inter system crossing pathway 295 in quinoline-pyrazole isomerism: a time-dependent density functional theory study on excited-state intramolecular proton transfer. *J. Phys. Chem. A*, 119, 6269-6274(2015).
 34. Liu Y. H., Mehata M. S. and Lan S. C., TDDFT study of the polarity controlled ion-pair separation in an excited-state proton transfer reaction, *Spectrochimica Acta A*, 128, 280-284(2014).
 35. Zhao J., Yao H., Liu J. and Hoffmann M. R., New excited-state proton transfer mechanisms for 1,8 dihydroxydibenzo[a, h] phenazine. *J. Phys. Chem A*, 119(4), 681-688(2015).
 36. Zhang M., and Zhao G. J., Modification of n-type organic semiconductor performance of perylene diimides by substitution in different positions: twodimensional pi-stacking and hydrogen bonding. *ChemSusChem*. 5(5), 879-887(2012).
 37. Zhao J., Chen J., Cui Y., Wang J., Xia L., Dai Y., Song P. and Ma P. F., A questionable excited-state double-proton transfer mechanism for 3-hydroxyisoquinoline, *Phys. Chem. Chem. Phys*, 17, 1142-1150(2015).
 38. Cheng C. L., and Zhao G. J., Steered molecular dynamics simulation study on dynamic self-assembly of single-stranded DNA with double-walled carbon nanotube and grapheme. *Nanoscale*, 4(7), 2301-2305(2012).
 39. McCarthy A. and Ruth A. A., Fluorescence excitation and excited state intra-molecular proton transfer of jet-cooled naphthol derivatives: part I. 1-hydroxy-2-naphthaldehyde, *Phys. Chem. Chem. Phys*, 13, 7485-7499(2011).
 40. Mondal S., Basu S. and Mandal D., Ground- and excited-state proton-transfer reaction of 3-hydroxyflavone in aqueous micelles. *Chem. Phys. Lett*, 479(4), 218-223(2009).
 41. Aein N. B. and Wan N. B.P., Excited state intramolecular proton transfer (ESIPT) from phenol OH (OD) to adjacent aromatic carbons in simple biphenyls, *J. Photochem. Photobiol*, 208, 42-49(2009).
 42. Huynh M. H. V. and Meyer T. J., Proton-Coupled Electron Transfer. *Chem. Rev*, 107(11), 5004-5064(2007).
 43. Gordon M. S., Freitag M. A., Bandyopadhyay P., Jensen J. H., Kairys V. and Stevens W. J., The Effective Fragment Potential Method: A QM-Based MM Approach to Modeling Environmental Effects in Chemistry. *J. Phys. Chem. A*, 105(2), 293-307(2001).
 44. Adamovic I., Freitag M. A. and Gordon M. S., Density functional theory based effective fragment potential method. *J. Chem. Phys*, 118(5), 6725-1732(2003).
 45. Ramegowda M., Change in energy of hydrogen bonds upon excitation of 6-aminocoumarin: TDDFT/EFP1 study. *New J. Chem*, 37(9), 2648-2653.
 46. Ramegowda M., A TDDFT/EFP1 study on hydrogen bonding dynamics of coumarin 151 in

- water. *Spectrochimica Acta Part A*, 137, 99-104(2015).
47. Hanwell M. D., Curtis D. E., Lonie D. C., Vandermeersch T., Zurek E. and Hutchison G. R., Avogadro: An advanced semantic chemical editor, visualization and analysis platform. *Aust. J. Chem*, 4(17), 1-14(2012).
 48. Glendening E. D., Landis C. R. and Weinhold F., Natural Bond Orbital Methods. *WIREs Comput. Mol. Sci*, 2, 1-42(2012).
 49. Schmidt M. W., Baldrige K. K., Boatz J. A., Elbert S. T., Gordon M. S., Jensen J. H., Koseki S., Matsunaga N., Nguyen K. A., Su S. J., Windus T. L., Dupuis M, and Montgomery J. A., General Atomic and Molecular Electronic Structure System. *J. Comput. Chem*, 14(11), 1347-1363(1993).
 50. Gordon M. S. and Schmidt M. W., *Advances in Electronic Structure Theory: GAMESS a Decade Later. Theory and Applications of Computational Chemistry: The First Forty Years*, Elsevier, Amsterdam, 1, 1167-1189(2005).
 51. Kohn W., Becke A. D. and Parr R. G., Density Functional Theory of Electronic Structure. *J. Phys. Chem*, 100(31), 12974-12980(1996).
 52. Kim K. and Jordan K. D., Comparison of Density Functional and MP2 Calculations on the Water Monomer and Dimer. *J. Phys. Chem*, 98(40), 10089-10094(1994).
 53. Stephens P. J., Devlin F. J., Chabalowski C. F. and Frisch M. J., Ab Initio Calculation of Vibrational Absorption and Circular Dichroism Spectra Using Density Functional Force Fields. *J. Phys. Chem*, 98(45), 11623-11627(1994).
 54. Stevens W. H., Basch H., Krauss M. and Jasien P., An effective fragment method for modeling solvent effects in quantum mechanical calculations. *The Journal of Chemical Physics*, 105(5), 1968-1986(1996).
 55. Cundari T. R. and Stevens W. J., Effective core potential methods for the lanthanides. *J. Chem. Phys*, 98(7), 5555-5565(1993).
 56. Hay P. J. and Wadt W. R., Ab initio effective core potentials for molecular calculations. Potentials for the transition metal atoms Sc to Hg. *J. Chem. Phys*, 82(1), 270-283(1985).
 57. Becke A. D., Development and assessment of new exchange-correlation functional. *J. Chem. Phys*, 109(15), 6264-1671(1998).
 58. Tokura S., Sato T., Tsuneda T., Nakajima T. and Hirao K. J., A dual-level state-specific time-dependent density-functional theory. *Comput Chem*, 29(8), 1187-1197(2008).
 59. Mahito C., Takao T. and Kimihiko H., Excited state geometry optimizations by analytical energy gradient of long-range corrected time-dependent density functional theory. *The journal of chemical physics*, 124(14), 144106-11(2006).
 60. Becke A. D., Density-functional exchange-energy approximation with correct asymptotic behavior. *Phys. Rev. A*, 38, 3098-3100(1998).
 61. Furche F. and Ahlrichs R., Erratum: "Time-dependent density functional methods for excited state properties". *J. Chem. Phys*, 121(24), 12772-12773(2004).
 62. Dejun Si. and Hui L., Analytic energy gradient in combined time-dependent density functional theory and polarizable force field calculation. *J. Chem. Phys.*, 133(14), 144112-8(2010).
 63. Perdew J., Ernzerhof M. and Burke K., Rationale for mixing exact exchange with density functional approximations. *J. Chem. Phys*, 105(22), 9982-1985(1996).
 64. Hariharan P. C. and Pople J. A., The influence of polarization functions on molecular orbital hydrogenation energies. *Theor. Chim. Acta*, 28, 213-222(1973).